Hydro

Measurements of Hydrodynamic Forces on a Two-Dimensional Impeller and a Modified Centrifugal Pump

by

Ron Franz and Norbert Arndt

California Institute of Technology
Pasadena, California 91125

July 1986

Report No. E249.4

Contract: NAS 8-33108

Approved: A.J. Acosta
C.E. Brennen
T.K. Caughey

NOMENCLATURE

$[A]$ = hydrodynamic force matrix, non-dimensionalized by $\rho\pi\omega^2 r_2^2 b_2$

A_2 = impeller outlet area ($2\pi r_2 b_2$)

b_2 = impeller discharge width (0.62 in)

$\{F\}$ = 6-component generalized force vector

F_1, F_2 = components of the instantaneous lateral force on the impeller in the rotating dynamometer reference frame

F_x, F_y = components of the instantaneous lateral force on the impeller in the fixed laboratory reference frame (X,Y), non-dimensionalized by $\rho\pi\omega^2 r_2^3 b_2$

F_{ox}, F_{oy} = values of F_x and F_y if the impeller was located at the the origin of the (X,Y) coordinate system (volute center), non-dimensionalized by $\rho\pi\omega^2 r_2^3 b_2$

F_n, F_t = components of the lateral force on the impeller normal to and tangential to the whirl orbit, averaged over the orbit, non-dimensionalized by $\rho\pi\omega^2 r_2^2 b_2 \varepsilon$

I/J = ratio of whirl/impeller shaft speed

p_{t1}, p_{t2} = upstream, downstream total pressure

Q = flow rate

r_2 = impeller discharge radius (3.188 in.)

t = time

(X,Y) = fixed laboratory reference frame

x,y = instantaneous coordinates of the impeller center in the fixed laboratory reference frame (X,Y), non-dimensionalized by r_2

ε = radius of the circular whirl orbit

θ = angle of the impeller on the eccentric circle, measured from the volute tongue in the direction of impeller rotation

ρ = density of water

ϕ = flow coefficient based on the impeller discharge area and tip speed, $\frac{Q}{\omega r_2 A_2}$

Φ = total head cofficient, $\frac{p_{t2}-p_{t1}}{\rho\omega^2 r_2^2}$

ω = radian frequency of the impeller (shaft) rotation

Ω = radian frequency of the whirl motion = $I\omega/J$

INTRODUCTION

Previously force measurements have been made on a centrifugal pump impeller [1,2]. The test section inlet of these tests was modified by increasing the volume of the annular region surrounding the shroud. Force meaurements were subsequently made on this modified configuration. In addition, a two dimen-

sional model of the impeller was tested.

The references [1,2] provide a description of the facility prior to the current modifications. Briefly, the dynamometer, composed of two parallel plates connected by four strain gaged posts, is mounted between the impeller and the drive shaft. It measures the six components of a generalized hydrodynamic force vector {F} acting on the impeller. The impeller is made to whirl in an orbit eccentric to the volute center, in addition to the normal shaft rotation. Since the eccentric motion is in the lateral plane, perpendicular to the impeller centerline, only the two components of the force vector {F} in this lateral plane will be discussed.

Refering to Fig. 1, these forces, in the stationary volute frame of reference, can be represented by

$$\begin{Bmatrix} F_x \\ F_y \end{Bmatrix} = \begin{Bmatrix} F_{ox} \\ F_{oy} \end{Bmatrix} + [A\,(\Omega/\omega)] \begin{Bmatrix} \varepsilon/r_2\ \cos\Omega t \\ \varepsilon/r_2\ \sin\Omega t \end{Bmatrix} \qquad (1)$$

The lateral forces, represented by F_x and F_y, can be considered as the sum of two forces: a fixed force, represented by F_{ox} and F_{oy}, which the impeller would experience if located at the volute center, and an unsteady force due to the eccentric motion of the impeller, represented by a force matrix [A]. The gravitational and bouyancy forces on the rotor are subtracted out. Dimensionless quantities are used throughout (see Nomenclature for definitions).

The data presented in this paper are derived from measurements with the impeller whirling in the circular orbit. When there is no whirl the matrix [A] and vector $\{F_o\}$ can still be extracted from measurements taken at four fixed eccentric positions, 90 degrees apart, except that these results are limited to the zero whirl value. In general, the force matrix [A] is a strong function of

the whirl speed ratio Ω/ω.

EXPERIMENTS

Force measurements of a centrifugal impeller (impeller X), a five bladed Byron-Jackson centrifugal impeller with a specific speed of 0.57, in a spiral volute (volute A) for various impeller speeds and flow rates have been made using the dynamometer [1,2].

Subsequently with the impeller shaft at fixed positions on its eccentric orbit, pressure measurements were taken at the volute entrance and in the annular region around the shroud [3-4]. During this program, the inlet flange of the test section was shortened. This modification exposed the annular region to the housing reservior, as shown in figure 2. The forces on impeller X in this modified test section were measured. Some of these results have already been reported [3-4]. During these tests, rings were installed within the volute with an axial clearance of .005 in. from the impeller to reduce leakage flow.

Impeller Z, a two-dimensional model of impeller X, figure 3, was constructed and installed in volute A. The inlet section was modified again, eliminating the annular region, figure 4. Throughout the above tests, the face seal clearances at the front and back of the impeller was .005 in.

RESULTS

The steady force $\{F_o\}$ as a function of flow coefficient is plotted in figure 5 for various tests. Included are previous results of impeller X in volute A without and with the rings before the modification, the inlet flange shortening. For impeller X the magnitude is smaller in the configuration with the

front flange shortened than the other configurations. Impeller Z has the smallest magnitude. For each impeller the steady force has a minimum. For flow coefficients below design, the direction of the force is at an angle above the tongue, in the direction of impeller shaft rotation. For higher flow coefficients, the force direction is below the tongue.

The diagonal elements of the hydrodynamic force matrix $[A(\Omega/\omega)]$ are nearly equal and the off-diagonal elements are nearly equal but of opposite sign. The matrix will be presented in terms of the average normal and tangential force, F_n and F_t, given by

$$F_n = (A_{xx} + A_{yy})/2 \quad \text{and} \quad F_t = (-A_{xy} + A_{yx})/2$$

F_n and F_t for the various configurations are compared in figures 6-7 for a flow coefficient of 0.06. Under reverse whirl both F_n and F_t for impeller X are smallest when installed in the modified test section. As F_n decreases the curves coalesce around $\Omega/\omega=.5$ where F_n is negative. F_t is in the same direction as the whirl motion, thus destabilizing, over a smaller range of whirl ratio. The forces on impeller Z are smaller. The projected area of the impeller exterior surface in the radial direction, upon which a pressure unbalance gives a lateral force, is smaller for impeller Z. Under reverse whirl the differences in F_n and F_t between impellers are clear. Under forward whirl, for $\Omega/\omega \leq 1.1$, the forces are smaller, so the difference is not outstanding.

The dependence of F_n and F_t on flow coefficient for impeller X with the front flange shortened is indicated in figures 8-9. Similarly figures 10-11 indicate their dependence for impeller Z.

CONCLUSION

The modification to the inlet flange, exposing the annular region surrounding the impeller shroud to the housing reservior, reduced the forces upon the centrifugal impeller X, and reduced the range of whirl ratios over which the average tangential force is destabilizing. These results show the importance of the external shrouds on the forces exerted on this impeller.

The two-dimensional model of impeller X, impeller Z, had a smaller steady force and a hydrodynamic force matrix with smaller elements. The average tangential force was destabilizing over a whirl ratio range comparable with impeller X in the unmodified test section with rings installed in the volute to reduce flow leakage.

REFERENCES

1. Jery, B., Brennen, C.E., Caughey, T.K., and Acosta, A.J., "Forces on Centrifugal Pump Impellers," "Second International Pump Symposium", Houston, Texas, April 29-May 2, 1985.

2. Jery, B., "Experimental Study of Unsteady Hydrodynamic Force Matrices on Whirling Centrifugal Pump-Impellers", Ph.D. Thesis, Division of Engineering and Applied Science, California Institute of Technology, October 1985.

3. Adkins D., "Analyses of Hydrodynamic Forces on Centrifugal Pump Impellers", Ph.D. Thesis, Division of Engineering and Applied Science, California Institute of Technology, December 1985.

4. Adkins, D., Brennen, C.E., "Analyses of Hydrodynamic Radial Forces on Centrifugal Pump", Fourth Rotordynamic Instability Problems in High Perfor-

mance Turbomachinery Workshop, Houston, Texas, June 2-4, 1986.

LIST OF FIGURES

Figure 1. Schematic representation of the lateral forces in the rotating dynamometer frame (as F_1,F_2), in the stationary volute frame (as F_x,F_y) and in the local polar coordinate frame (as F_n,F_t).

Figure 2. Assembly drawing of impeller X in the modified test section, with the inlet flange shortened.

Figure 3. Drawing of impeller Z, a two-dimensional model of impeller X.

Figure 4. Assembly drawing of impeller Z installed in the test section.

Figure 5. The magnitude and direction of the steady force $\{F_o\}$ as a function of flow coefficient at 1000 RPM of impeller X in volute A without flow leakage rings, with rings, and also with the front flange shortened and of impeller Z in volute A.

Figure 6. Average normal force at 1000 RPM with a flow coefficient of 0.06 of impeller X in volute A without flow leakage rings, with rings, and also with the front flange shortened and of impeller Z in volute A.

Figure 7. Average tangential force at 1000 RPM with a flow coefficient of 0.06 of impeller X in volute A without flow leakage rings, with rings, and also with the front flange shortened and of impeller Z in volute A.

Figure 8. Average normal force at 1000 RPM of impeller X in volute A with flow leakage rings in the modified test section, front flange shortened, for various flow coefficients.

Figure 9. Average tangential force at 1000 RPM of impeller X in volute A with flow leakage rings in the modified test section, front flange shortened, for various flow coefficients.

Figure 10. Average normal force at 1000 RPM of impeller Z in volute A for various flow coefficents.

Figure 11. Average tangential force at 1000 RPM of impeller Z in volute A for various flow coefficents.

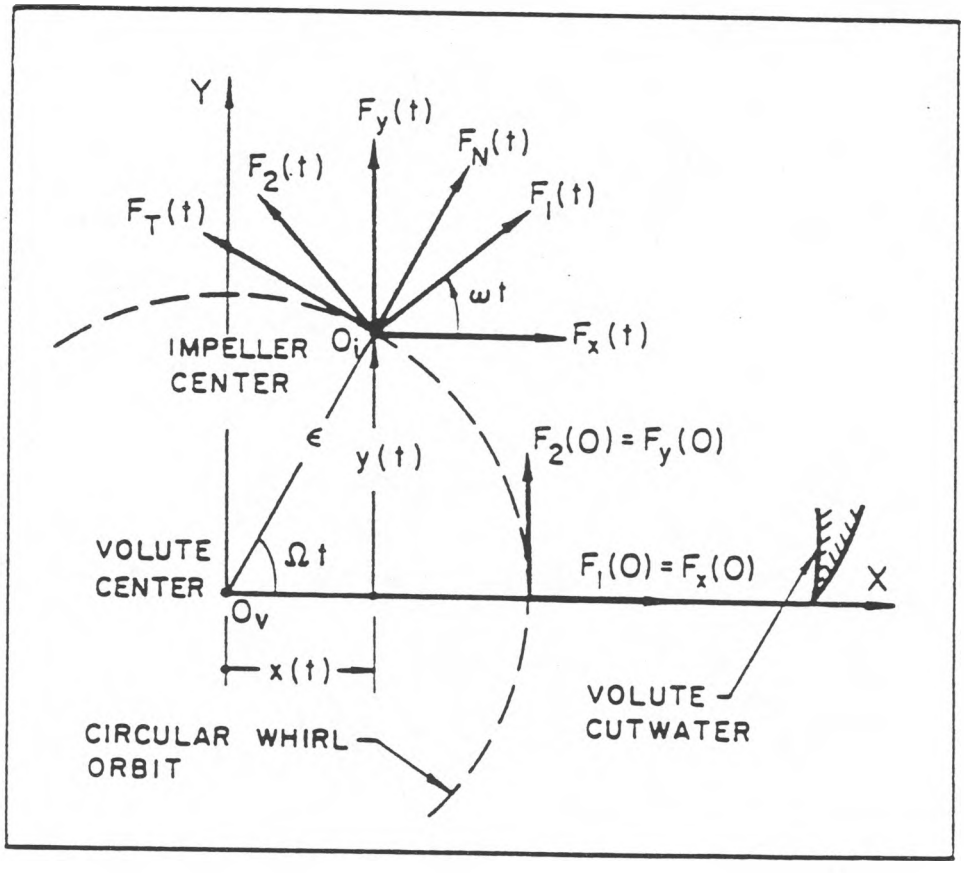

Figure 1. Schematic representation of the lateral forces in the rotating dynamometer frame (as F_1,F_2), in the stationary volute frame (as F_x,F_y) and in the local polar coordinate frame (as F_n,F_t).

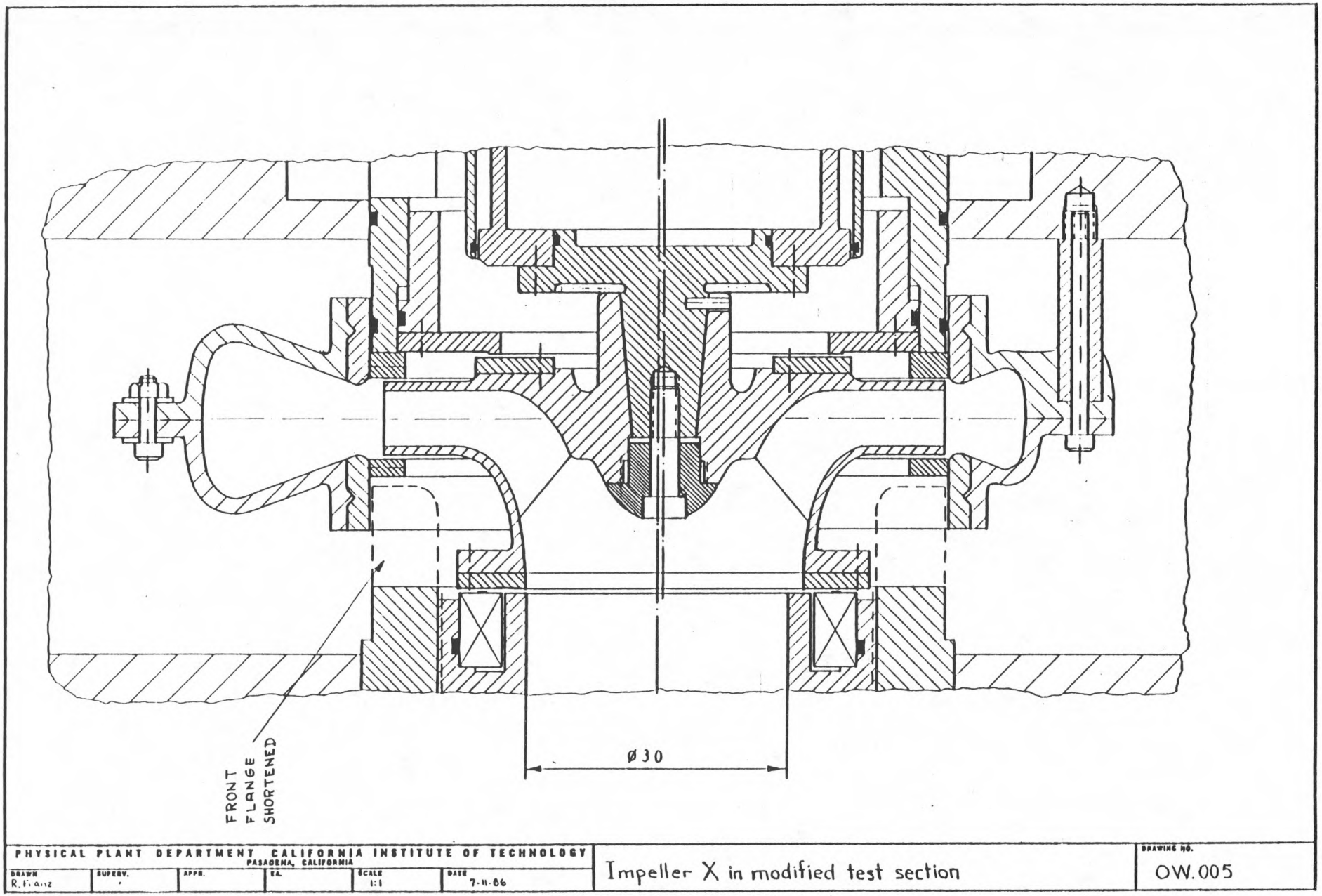

Figure 2. Assembly drawing of impeller X in the modified test section, with the inlet flange shortened.

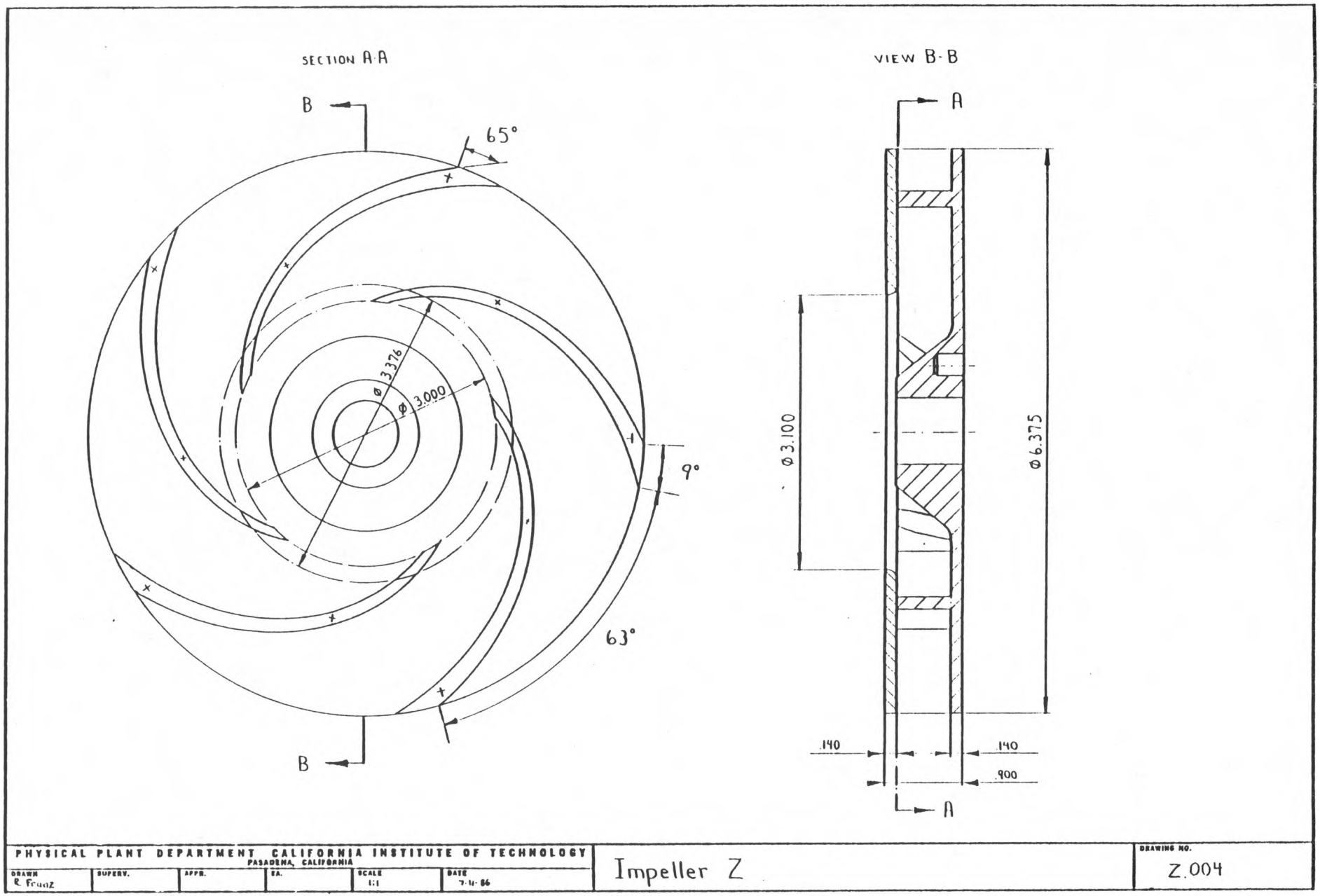

Figure 3. Drawing of impeller Z, a two-dimensional model of impeller X.

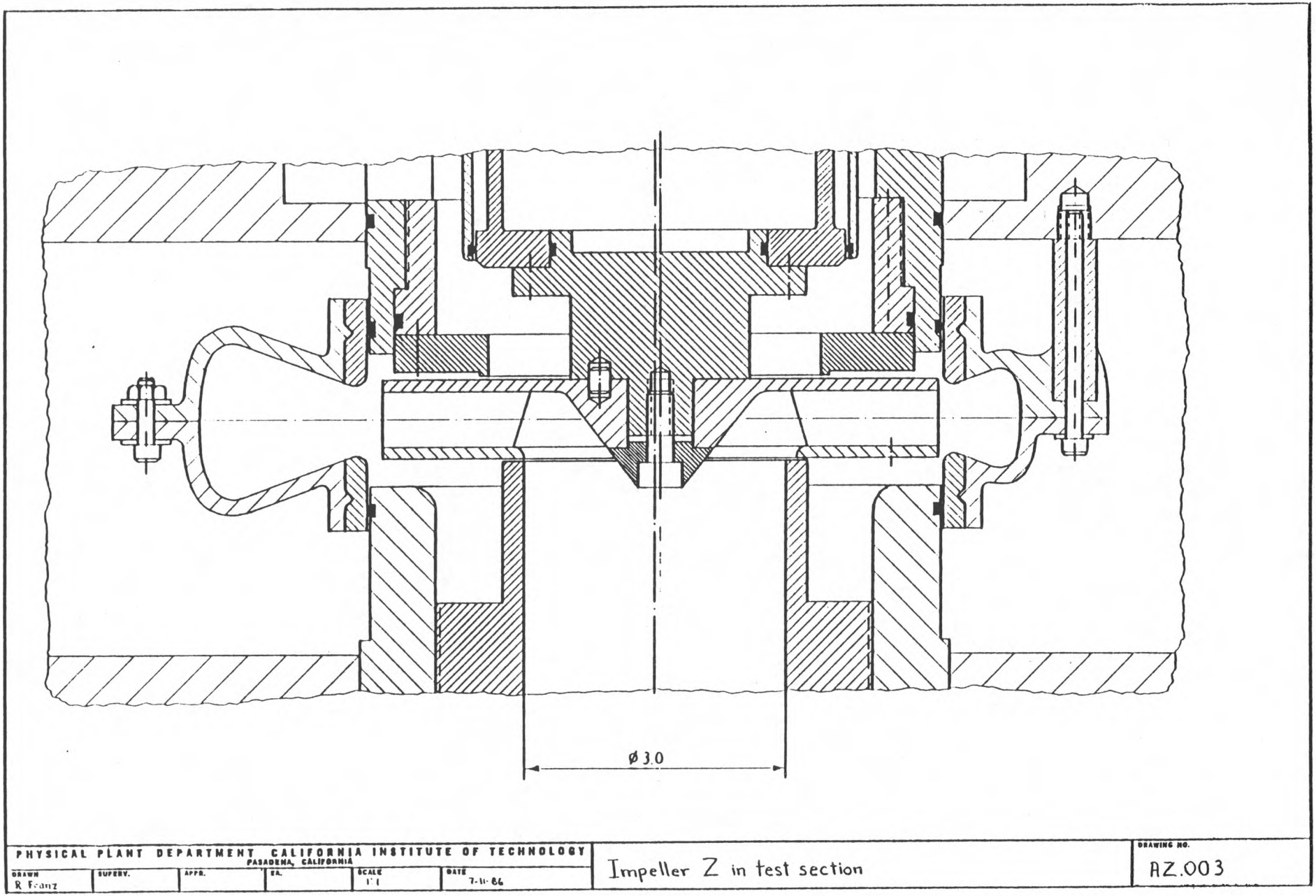

Figure 4. Assembly drawing of impeller Z installed in the test section.

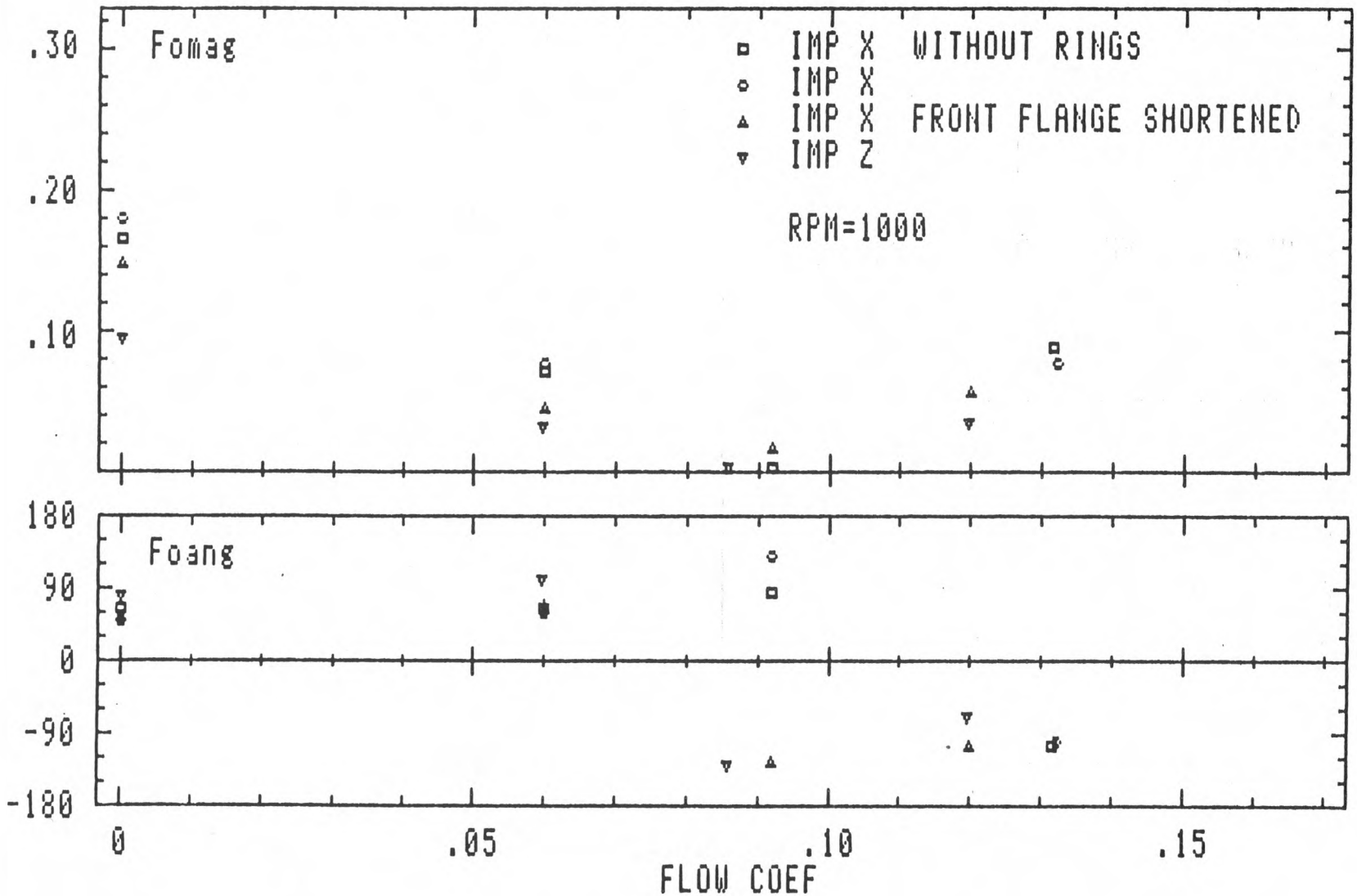

Figure 5. The magnitude and direction of the steady force (F_o) as a function of flow coefficient at 1000 RPM of impeller X in volute A without flow leakage rings, with rings, and also with the front flange shortened and of impeller Z in volute A.

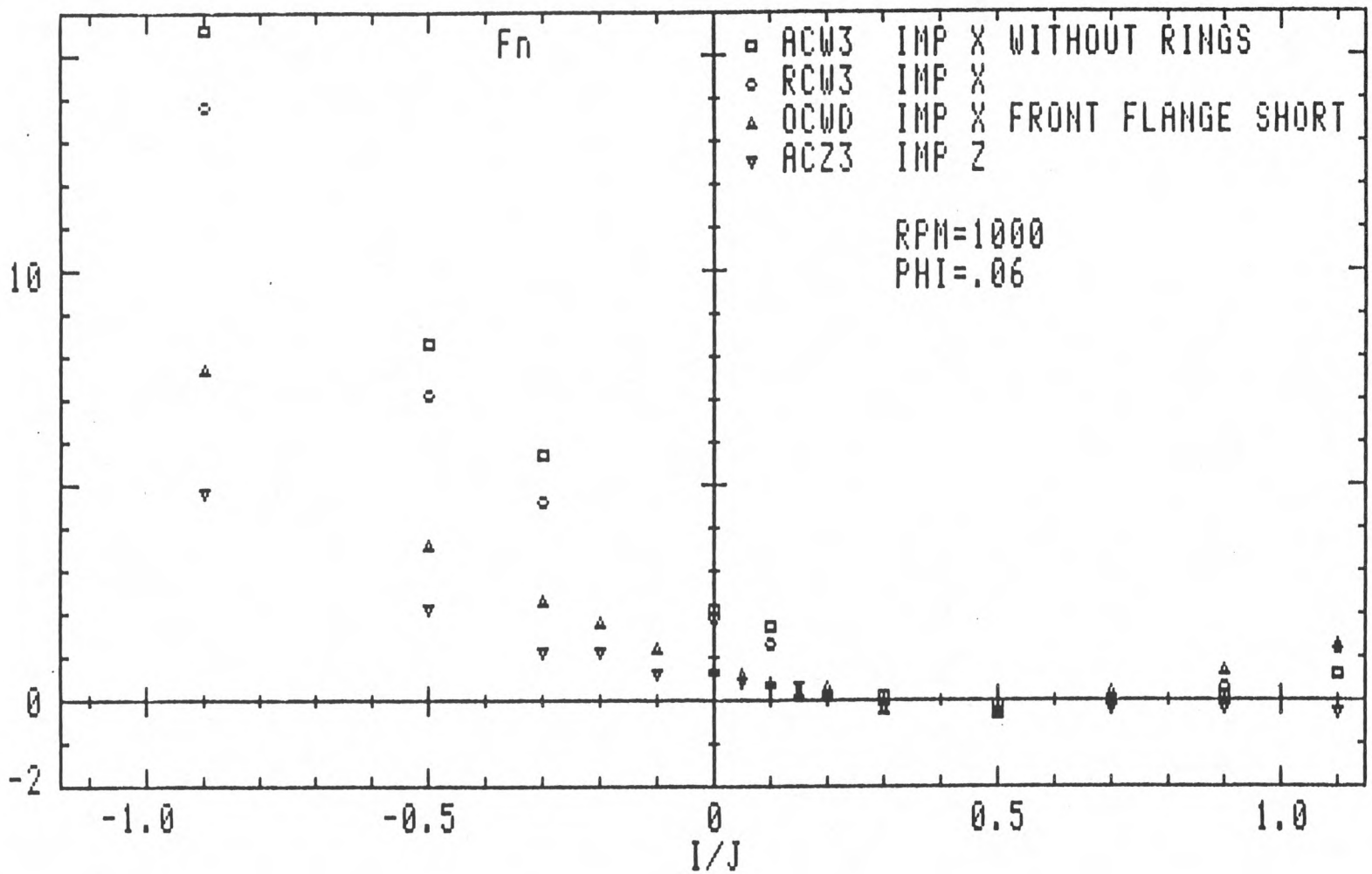

Figure 6. Average normal force at 1000 RPM with a flow coefficient of 0.06 of impeller X in volute A without flow leakage rings, with rings, and also with the front flange shortened and of impeller Z in volute A.

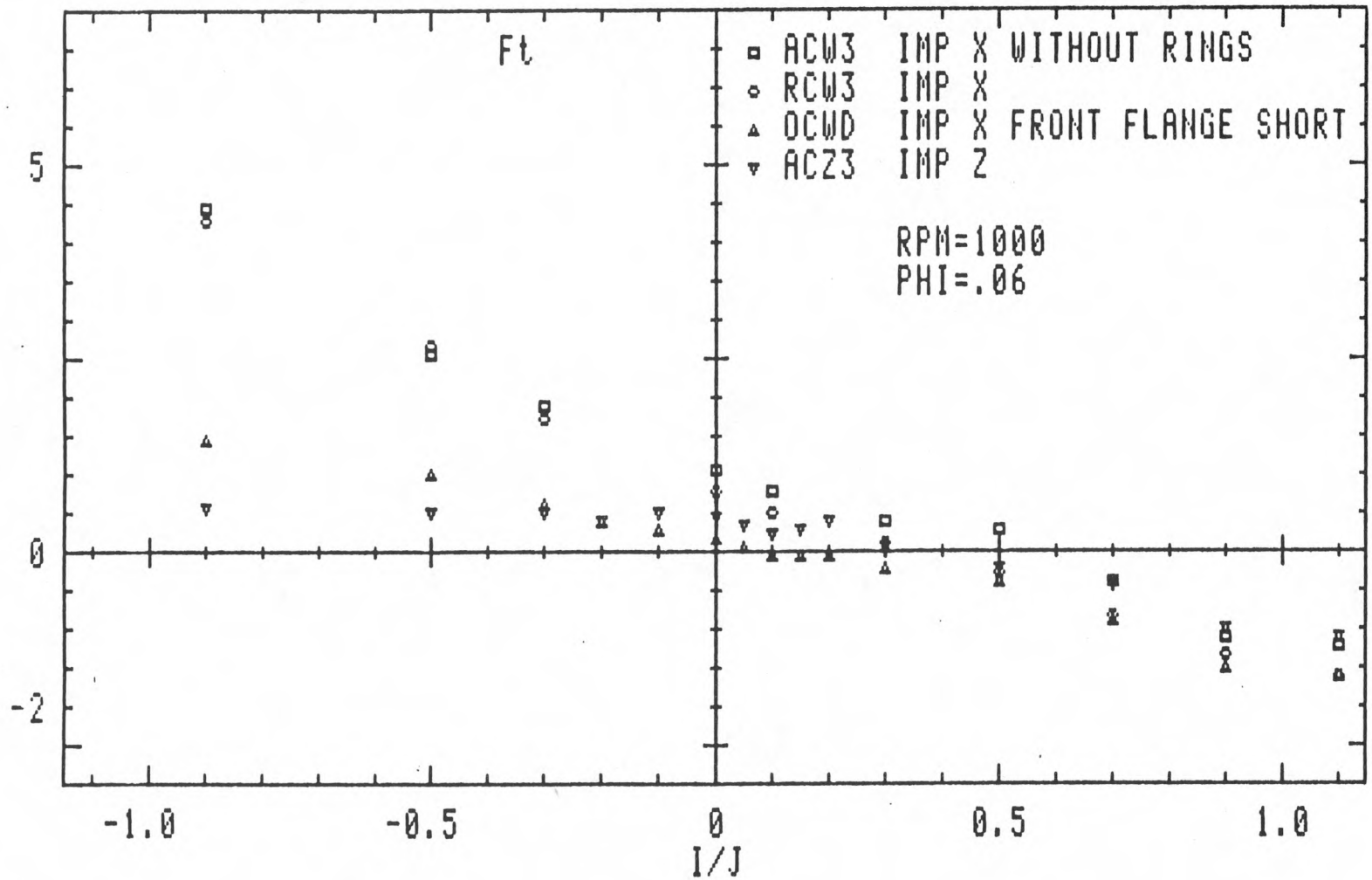

Figure 7. Average tangential force at 1000 RPM with a flow coefficient of 0.06 of impeller X in volute A without flow leakage rings, with rings, and also with the front flange shortened and of impeller Z in volute A.

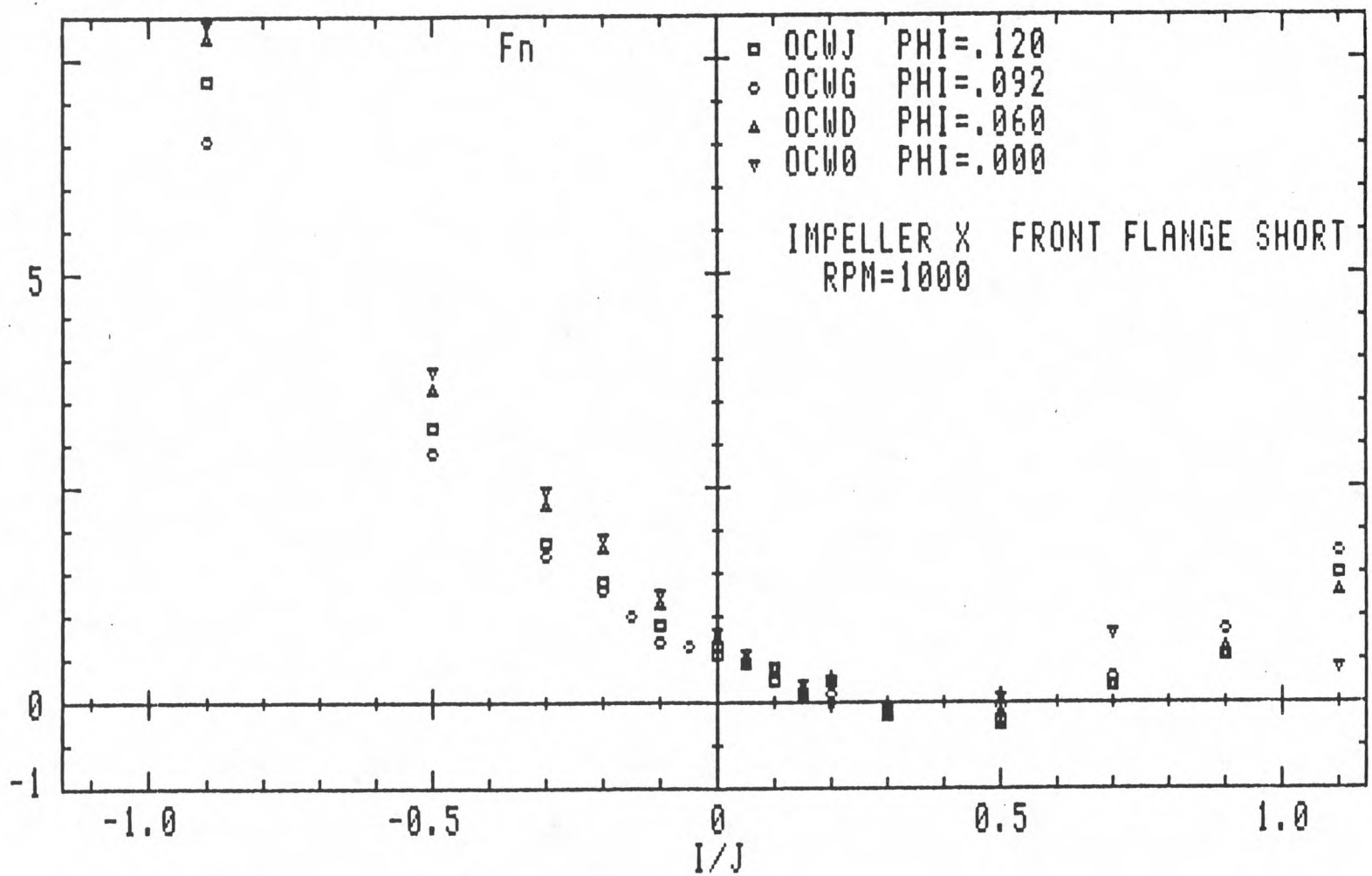

Figure 8. Average normal force at 1000 RPM of impeller X in volute A with flow leakage rings in the modified test section, front flange shortened, for various flow coefficients.

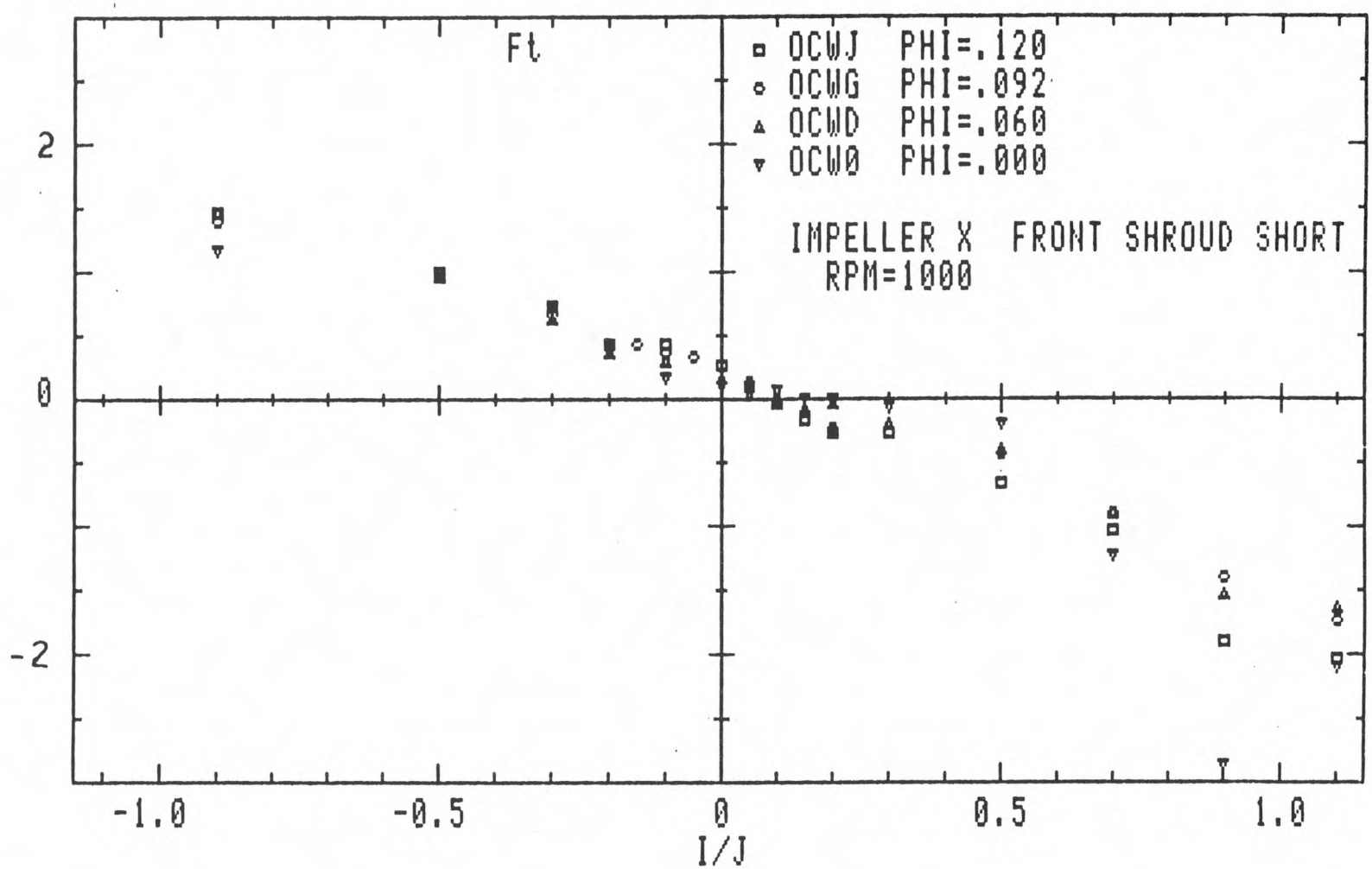

Figure 9. Average tangential force at 1000 RPM of impeller X in volute A with flow leakage rings in the modified test section, front flange shortened, for various flow coefficients.

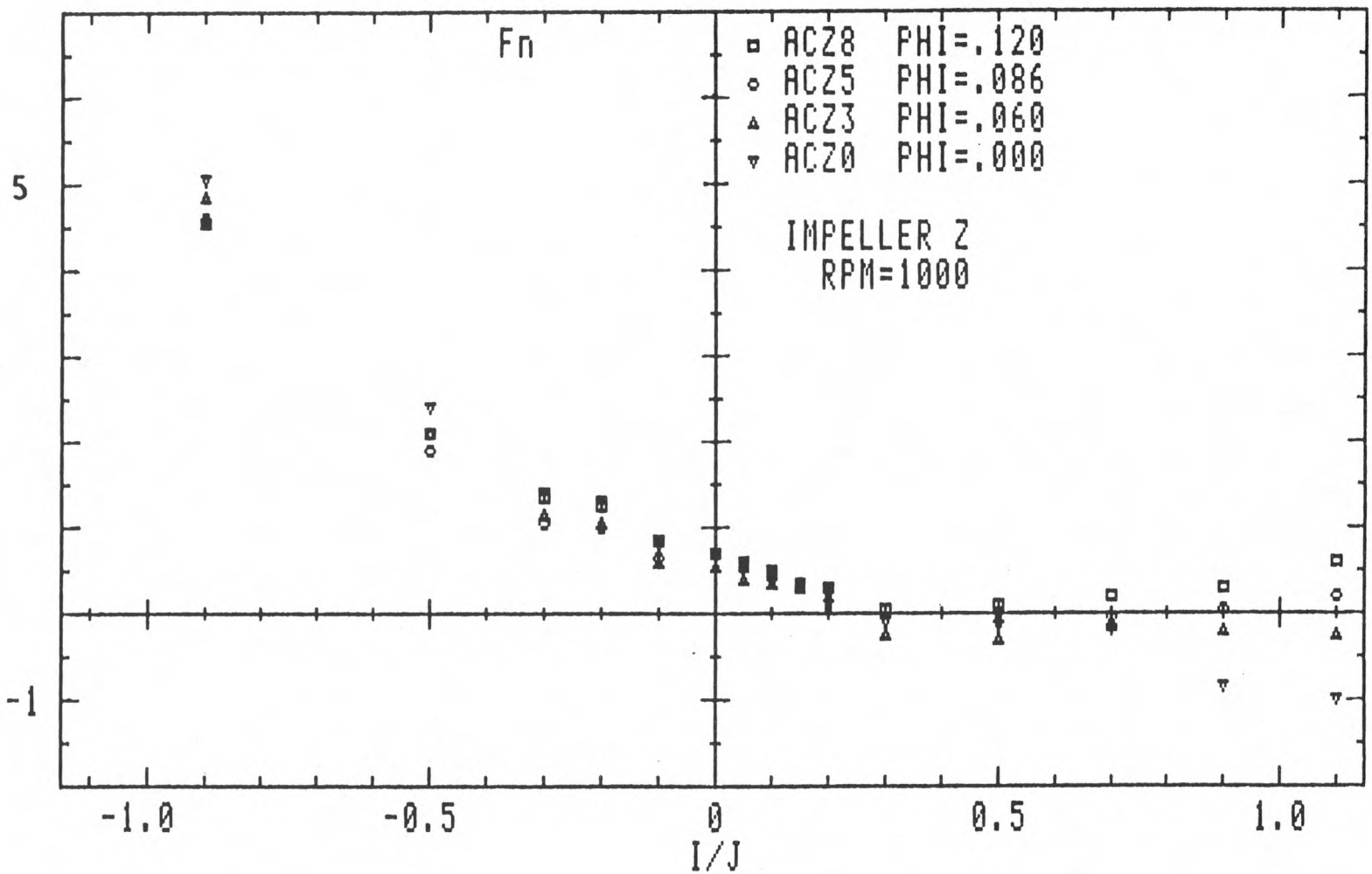

Figure 10. Average normal force at 1000 RPM of impeller Z in volute A for various flow coefficents.

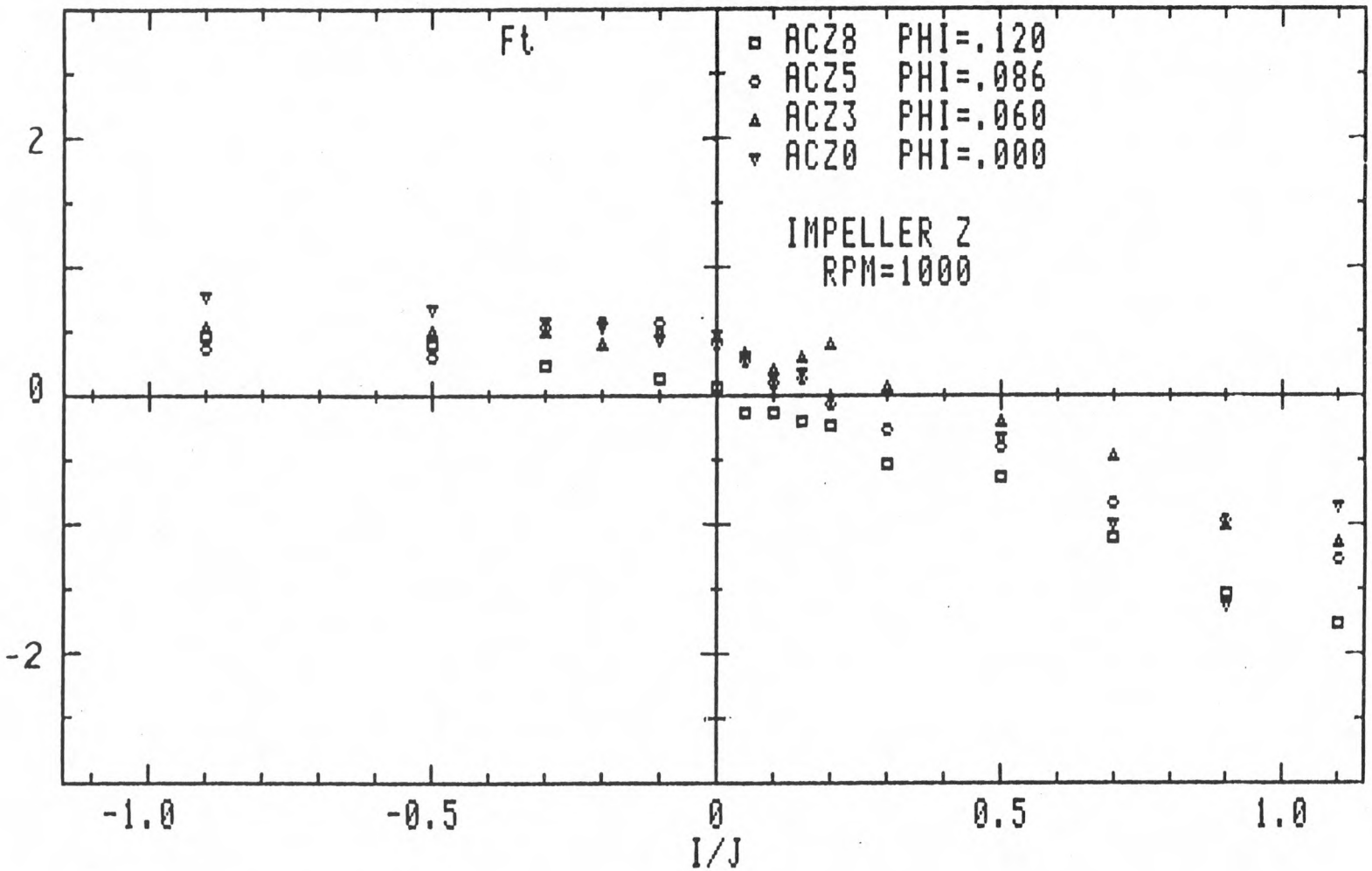

Figure 11. Average tangential force at 1000 RPM of impeller Z in volute A for various flow coefficents.